Fuel 159 (2015) 98–106

Contents lists available at ScienceDirect

Fuel

journal homepage: www.elsevier.com/locate/fuel

Laminar burning velocity and Markstein length of ammonia/air premixed flames at various pressures

Akihiro Hayakawa *, Takashi Goto, Rentaro Mimoto, Yoshiyuki Arakawa, Taku Kudo, Hideaki Kobayashi

Institute of Fluid Science, Tohoku University, 2-1-1 Katahira, Aoba-ku, Sendai, Miyagi 980-8577, Japan

HIGHLIGHTS

- Laminar burning velocities of ammonia/air flames at high pressures are evaluated.
- Maximum value of laminar burning velocity of ammonia/air flame is about 7 cm/s.
- Laminar burning velocity decreases with the increase in the pressure.
- Markstein length increases with the increase in equivalence ratio.
- Markstein lengths at high pressure are lower than those at 0.1 MPa.

ARTICLE INFO

Article history:
Received 24 February 2015
Received in revised form 12 June 2015
Accepted 20 June 2015
Available online 28 June 2015

Keywords:
Laminar flames
Ammonia
High pressure
Burning velocity
Markstein length
Numerical simulation

ABSTRACT

Ammonia is expected to be useful not only as a hydrogen-energy carrier but also as a carbon-free fuel. In order to design an ammonia fueled combustor, fundamental flame characteristics of ammonia must be understood. However, knowledge of the characteristics of ammonia/air flames, especially at the high pressures, has been insufficient. In this study, the unstretched laminar burning velocity and the Markstein length of ammonia/air premixed flames at various pressures up to 0.5 MPa were experimentally clarified for the first time. Spherically propagating premixed flames, which propagate in a constant volume combustion chamber, were observed using high-speed schlieren photography. Results indicate that the maximum value of unstretched laminar burning velocities is less than 7 cm/s within the examined conditions and is lower than those of hydrocarbon flames. The unstretched laminar burning velocity decreases with the increase in the initial mixture pressure, tendency being the same as that of hydrocarbon flames. The burned gas Markstein length increases with the increase in the equivalence ratio, the tendency being the same as that of hydrogen/air flames and methane/air flames. The burned gas Markstein lengths at 0.1 MPa are higher than those at 0.3 MPa and 0.5 MPa. However, the values of burned gas Markstein length at 0.3 MPa and 0.5 MPa are almost the same. In addition, numerical simulations using CHEMKIN-PRO with five detailed reaction mechanisms which are presently applicable for the ammonia/air combustion were also conducted. However, qualitative predictions of unstretched laminar burning velocity using those reaction mechanisms are inaccurate. Thus, further improvements of reaction mechanisms are essential for application of ammonia/air premixed flames.

1. Introduction

Ammonia holds promise as a hydrogen energy carrier because of its high hydrogen weight of 17.7% [1]. At present, ammonia is widely used as a fertilizer. Application of ammonia as a hydrogen energy carrier would be useful because the infrastructure for ammonia distribution has already been established and the ammonia production process, i.e., the Haber–Bosch process, is well-known. Recently, a new process for producing ammonia by utilizing renewable energy sources, such as solar energy, is being studied [2]. In addition, ammonia also shows promise as a carbon-free fuel. However, in general, because of its lower combustion intensities, which means lower calorific value, slower laminar burning velocity and narrower flammability range, ammonia has not been considered as a fuel. Hence, fundamental flame characteristics of ammonia flame have been insufficiently studied.

In order to improve the lower combustion intensities of ammonia, hydrogen-added ammonia flames have been studied [3–7]. Lee et al. [3,4] experimentally investigated the laminar burning

* Corresponding author. Tel.: +81 22 217 5273; fax: +81 22 217 5323.
E-mail address: hayakawa@flame.ifs.tohoku.ac.jp (A. Hayakawa).

http://dx.doi.org/10.1016/j.fuel.2015.06.070
0016-2361/

velocity of hydrogen-added ammonia/air premixed flames. They showed the laminar burning velocity and Markstein numbers at the atmospheric pressure and clarified that the laminar burning velocity increases and the Markstein number decreases with an increase in hydrogen concentration. Kumar and Meyer [5] showed the laminar burning velocity of hydrogen/ammonia/air flames by considering the heat loss from the flames. The application of ammonia in an actual combustor is also being studied. Frigo et al. [6,7] applied hydrogen-doped ammonia as a fuel for the spark ignition engines. The power and thermal efficiencies of a hydrogen-doped ammonia fielded engine were compared with those of a gasoline engine. In addition, consideration is being given to on-board cracking of ammonia in order to obtain hydrogen as a flame promoter in SI engines.

Recently, flame characteristics of ammonia/air premixed flames have been studied. Hayakawa et al. [8] experimentally and numerically investigated premixed ammonia/air laminar flames at atmospheric pressure as well as at elevated pressures. Experimental and numerical observations showed that the NO formation from ammonia/air flames was reduced in rich mixtures because of the reduction NO by ammonia. In addition, it was also clarified that NO formation decreases with an increase in pressure due to the enhancement of consumption of H and OH radicals, which play an important role in NO formation.

Detailed reaction mechanisms of ammonia flames have been developed by Miller et al. [9] and Lindstedt et al. [10], and reaction mechanisms of C reactions, including N chemistry, are also available for ammonia combustion as proposed by Konnov [11] and Tian et al. [12]. However, since these mechanisms were not elucidated based on ammonia/air flames, it is unclear whether they are applicable for ammonia/air flames owing to insufficiency of experimental results for ammonia/air combustion.

Laminar burning velocity is one of the most important parameters for premixed flames and for confirmation of reaction mechanisms. The laminar burning velocities of ammonia/air premixed flames have been investigated by Zakaznov et al. [13], Takizawa et al. [14] and Pfahl et al. [15]. According to their results, the laminar burning velocity of ammonia/air premixed flames is lower than that of hydrocarbon flames, such as methane/air flames and propane/air flames. In studies of Takizawa et al. [14] and Pfahl et al. [15], spherically propagating flames in a constant volume combustion chamber were investigated for the evaluation of laminar burning velocity. Although flame stretch, which causes a change in flame speed owing to thermo-diffusive effects [16], was known to occur for spherically propagating laminar flames, the effects of flame stretch on flame speed were not considered in these studies. In addition, all experiments were conducted at atmospheric pressure.

Spherically propagating premixed flames in a constant volume combustion chamber have been widely investigated in order to clarify the fundamental characteristics of premixed flames [17–20]. Kitagawa and Hayakawa et al. [17,18] investigated spherically propagating laminar and turbulent flames in a large constant volume combustion chamber for hydrogen and iso-octane up to initial mixture pressure of 0.5 MPa. Tse et al. [19] investigated flame propagation up to 60 atm using two concentric cylindrical vessels. Kelley et al. [20] proposed a non-linear relationship between flame speed and flame stretch rate.

The Markstein length and the Markstein number are also important parameters for laminar flames because these values express the role of thermo-diffusive effects. Although these values are important for laminar flame characteristics, such as flame instability [21], turbulent flame characteristics are also affected by the Markstein length or the Markstein number. Hayakawa et al. [18] investigated the turbulent burning velocity at fixed turbulence Karlovitz numbers and showed that the ratio of turbulent burning velocity to unstretched laminar burning velocity increases with a decrease in Markstein number. Kobayashi et al. [22] proposed that the Markstein length affects the flame surface density of the turbulent flame front via a change in the passivity of the flame front. Bradley et al. [23] expressed the correlation between turbulent burning velocity and effective turbulence intensity. Therefore, evaluation of the Markstein length or the Markstein number is also important for an understanding of turbulent combustion.

The objectives of the present study were to evaluate the laminar burning velocity and the Markstein length of ammonia/air premixed flames at various pressures up to 0.5 MPa. The equivalence ratios were varied from 0.7 to 1.3. In addition, numerical simulations using various detailed reaction mechanisms were also carried out. The results of numerical simulations are compared with the experimental results in the next sections.

2. Experimental setup and numerical method

Fig. 1 shows the experimental setup used in this study. Experiments were carried out using a constant volume cylindrical combustion chamber. The inner diameter and length of the chamber were 270 mm and 410 mm, respectively. The volume of the chamber was approximately 23 L, equivalent to that of a sphere with a diameter of 355 mm. The mixture was ignited by spark electrodes near the center of the chamber. The diameter of the spark electrodes was 1.5 mm and the spark gap was set to 2 mm.

A capacitor discharge ignition (CDI) circuit was adopted for spark ignition of the mixture. The electrostatic energy, which was charged in the capacitor in the CDI circuit, was set to 2.8 J. Although the energy of 2.8 J was different from the ignition energy and extremely larger than the minimum ignition energy of usual fuels, such as hydrocarbons [24], it was required to ensure the ignition of the ammonia/air mixture at atmospheric pressure. As described in Section 4.2, the ignition-affected regimes during flame propagation were not considered in the analysis of the determination of unstretched flame speed and Markstein length. Optical windows made of quartz glass were located opposite each other and flame propagation could be observed via these two windows.

Ammonia was used as the fuel and air was used as the oxidizer. Experimental conditions are summarized in Table 1. Initial mixture pressure, P_i, and the equivalence ratio, ϕ, were varied from 0.1 to 0.5 and 0.7 to 1.3, respectively. All experiments were conducted at a temperature of 298 K. The mixture was prepared according to the partial pressure of ammonia and air. The pressure inside of the chamber was measured by a pressure sensor (P1 in Fig. 1, GE Sensing UNIC5000). Experiments were carried out at least five times for each examined condition. The unstretched laminar burning velocity and burned gas Markstein length, which will be described in Section 4.2, were determined as the averaged value of the results obtained from each experiment. Experimental fluctuation was defined as the difference between maximum and minimum values of the experimental results. Schlieren photography with a high-speed camera and a continuous light source was adopted for the flame observation. A metal halide lamp (Photron, HVC-SL) and a high-speed camera (Photron, FASTCAM SA5) were used for the schlieren system. In order to form a spotlight source, a pinhole was mounted in front of the metal halide lamp. A micro lens (Nikon, Ai AF Micro-Nikkor 200mm f/4D IF-ED) was mounted on the high-speed camera. The resolution of the schlieren photography was 768 × 768 and the frame rate was 1000 fps. The resolution of the schrieren images was approximately 0.1 mm/pixel. Flame propagation could be obtained up to 60 mm in diameter using the schlieren technique via two optical windows. In addition, direct color high-speed photographs were taken by a high-speed

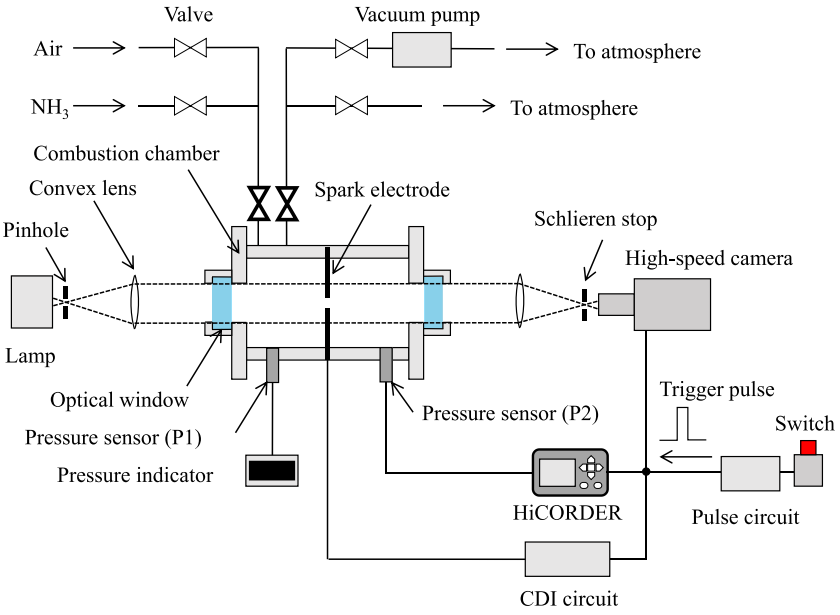

Fig. 1. Schematic of experimental setup.

Table 1
Examined conditions.

Equivalence ratio, ϕ (–)	0.7. 0.8, 0.9, 1.0, 1.1, 1.2, 1.3
Initial mixture pressure, P_i (MPa)	0.1, 0.3, 0.5
Initial mixture temperature (K)	298

camera (Photron, FASTCAM SA-Z) with a lens (Nikon, AF-S DX Nikkor 35mm f/1.8G). The resolution and frame rate of color imaging were 1024 × 1024 and 1000 fps, respectively. The spatial resolution of the direct image was approximately 0.2 mm/pixel.

The pressure inside of the chamber during flame propagation was measured by a pressure sensor (P2 in Fig. 1, Kyowa, PVL-10KD) and recorded by a memory recorder (HIOKI, MEMORY HiCORDER LR8431) with a sampling rate of 1 kHz. A pulse circuit was also adopted. When the switch was pushed, a single trigger pulse was outputted from the pulse circuit. The ignition timing of the mixture, recorded by the high-speed camera and the memory recorder started simultaneously.

Numerical simulations were also performed using a one-dimensional freely propagating laminar flame model of CHEMKIN-PRO [25]. The detailed chemical kinetics of Miller et al. [9], Lindstedt et al. [10], Konnov [11] without all carbon reactions, Tian et al. [12] and GRI-Mech 3.0 [26] were used in this study. The initial mixture temperature was set to 298 K. Pressure was varied from 0.1 to 0.5 MPa. In the case of numerical simulation, unstretched laminar burning velocity, S_L, was defined as the velocity at the cold boundary in the computational domain.

Table 2 shows the mixture and flame characteristics of ammonia/air premixed flames. Here, ρ_u and ρ_b are unburned mixture density and burned gas density, respectively. The densities were evaluated from the equilibrium calculation of CHEMKIN-PRO with thermo transport data of Tian et al. [12]. λ, c_p, α and ν are thermal conductivity, specific heat at constant pressure, thermal diffusivity and kinematic viscosity, respectively. The Lewis number of deficient components, *Le*, is also shown in Table 2. As shown in Table 2, the Lewis numbers of lean mixtures are lower than unity and almost constant for rich mixtures.

Table 2
Properties of ammonia/air mixtures used in the present study.

P_i (MPa)	ϕ (–)	ρ_u (kg/m^3)	ρ_b (kg/m^3)	λ (10^{-3} W/m/K)	c_p (J/kg/K)	α (10^{-5} m^2/s)	ν (10^{-5} m^2/s)	*Le* (–)
0.1	0.7	1.101	0.182	27.21	1121	2.205	1.575	0.95
	0.8	1.091	0.167	27.31	1135	2.205	1.575	0.94
	0.9	1.083	0.155	27.41	1149	2.204	1.575	0.94
	1.0	1.074	0.146	27.50	1162	2.203	1.576	=
	1.1	1.066	0.146	27.59	1175	2.203	1.576	1.09
	1.2	1.058	0.148	27.68	1188	2.202	1.576	1.09
	1.3	1.051	0.149	27.76	1200	2.201	1.576	1.09
0.3	0.7	3.302	0.546	27.21	1121	0.735	0.525	0.95
	0.8	3.274	0.501	27.31	1135	0.735	0.525	0.94
	0.9	3.248	0.465	27.41	1149	0.735	0.525	0.94
	1.0	3.222	0.437	27.50	1162	0.734	0.525	=
	1.1	3.198	0.438	27.59	1175	0.734	0.525	1.09
	1.2	3.175	0.443	27.68	1188	0.734	0.525	1.09
	1.3	3.152	0.448	27.76	1200	0.734	0.526	1.09
0.5	0.7	5.503	0.910	27.21	1121	0.441	0.315	0.95
	0.8	5.457	0.835	27.31	1135	0.441	0.315	0.94
	0.9	5.413	0.775	27.41	1149	0.441	0.315	0.94
	1.0	5.370	0.727	27.50	1162	0.441	0.315	=
	1.1	5.330	0.729	27.59	1175	0.441	0.315	1.09
	1.2	5.291	0.738	27.68	1188	0.440	0.315	1.09
	1.3	5.254	0.747	27.76	1200	0.440	0.315	1.09

3. Evaluation of laminar burning velocity and Markstein length

The laminar burning velocity and the Markstein length were obtained by the following methodology. The flame radius obtained from the schlieren image, r_{sch}, was determined to be the radius of a circle whose area was equivalent to the area of the schlieren image of spherically propagating flame. In the case of spherically propagating premixed flames, the flame speed during flame propagation, S_N, is evaluated by Eq. (1):

$$S_N = \frac{dr_{sch}}{dt}, \tag{1}$$

where t is time.

Because the spherically propagating premixed flame is curved at the flame front, the effects of flame stretch on flame

characteristics must be considered. The flame stretch rate, ε, is determined as the change in flame front area per unit area and unit time. In the case of spherically propagating flames, the flame stretch rate is derived by Eq. (2):

$$\varepsilon = \frac{1}{A}\cdot\frac{dA}{dt} = \frac{2}{r_{sch}}\cdot\frac{dr_{sch}}{dt}, \tag{2}$$

where A ($=4\pi r_{sch}^2$, for spherically flame) is the flame front area. In the case of non-unity Lewis number flames, thermo-diffusive effects occur, and thus flame temperature as well as laminar burning velocity are different from those of the unstretched flame. According to asymptotic analysis, the difference between unstretched flame speed, S_S, and stretched flame speed, S_N, can be considered to be proportional to the flame stretch rate, as shown by Eq. (3) [27]:

$$S_S - S_N = L_b \cdot \varepsilon, \tag{3}$$

where the proportional constant L_b is the burned gas Markstein length. Thus, the unstretched flame speed, S_S, can be determined by the extrapolation of $\varepsilon \to 0$ (or $r_{sch} \to \infty$). The unstretched laminar burning velocity, S_L, can then be calculated by Eq. (4):

$$S_L = \frac{\rho_b}{\rho_u}\cdot S_S. \tag{4}$$

Recently, Kelley and Law [20] proposed a non-linear relationship between the unstretched laminar burning velocity and the stretched laminar burning velocity. In this case, the linear approximation of Eq. (3) is available because the Lewis numbers of ammonia/air flames are close to unity, as shown in Table 2 [28].

4. Experimental results

4.1. Flame observation

Fig. 2 shows direct images of spherically propagating ammonia/air premixed laminar flame at elapsed time from the ignition, t, taken at 100 ms at an initial mixture pressure of 0.1 MPa at equivalence ratios of (a) $\phi = 0.8$, (b) $\phi = 1.0$ and (c) $\phi = 1.2$. Orange chemiluminescence was observed from ammonia/air premixed flames. Hayakawa et al. [8] proposed that the orange chemiluminescence was caused by the NH_2 ammonia α band spectra [29] and the superheated H_2O vapor spectra. NH_2 increases as the equivalence ratio increases, and orange chemiluminescence becomes clearer. The shape of flame at $\phi = 0.8$ was jellyfish-like at $t = 100$ ms. As described in Section 4.2, the unstretched laminar burning velocity at $\phi = 0.8$ is very low. Therefore, buoyancy is significantly influenced, especially for this condition, and consequently changes the flame shape.

Fig. 3 shows the pressure history inside the chamber, P, during flame propagation at $\phi = 1.0$ and $P_i = 0.1$ MPa. The increase of the pressure, within the observation range of 60 mm in diameter, was less than 2% from the initial mixture pressure, P_i, because the volume of the chamber is sufficiently large compared to the visible range of schlieren photography. Therefore, the pressure in the chamber during flame propagation can be assumed to be constant within the observation range.

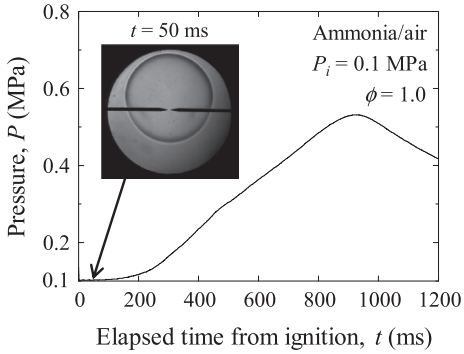

Fig. 3. Pressure history during flame propagation.

Fig. 4 shows schlieren images of ammonia/air premixed flames at various equivalence ratios, ϕ, with elapsed time from the ignition, t, at (a) $P_i = 0.1$ MPa, (b) $P_i = 0.5$ MPa, respectively. In the case of the equivalence ratio of 0.7 at $P_i = 0.1$ MPa, a hot gas regime generated by an electric spark could be observed between the spark electrodes at $t = 0$ ms. The boundary of the hot gas regime became obscure at $t = 40$ ms. After that, the boundary of the hot gas seems to disappear at $t = 80$ ms. This denotes that the flame does not propagate throughout the chamber under this condition. A similar phenomenon was also observed at $\phi = 1.3$ and at $P_i = 0.1$ MPa. The lean and rich flammability limits of ammonia flame are $\phi = 0.63$ and $\phi = 1.4$ [30], respectively, and present experimental results were close to the lean and rich flammability limits. However, flame propagates throughout the chamber at $P_i = 0.3$ MPa and 0.5 MPa at $\phi = 0.7$ and $\phi = 1.3$, respectively.

According to Paschen's law, voltage at the spark increases with an increase in initial mixture pressure. Ballal and Lefebvre [31] showed that the released energy of the electric spark increases with the increases in pressure if the spark gap remains constant. Although the ignition energy could not be evaluated in this study, it is considered to increase with an increase in the initial mixture pressure. In the case of equivalence ratios of 0.8, 1.0 and 1.2, spherically propagating premixed flame propagated throughout the chamber for all examined initial mixture pressure conditions. After 40 ms from ignition, the flame radius at $\phi = 1.0$ was larger than that at $\phi = 0.8$ and 1.2. The center of spherical flame was close to the gap of spark electrodes until $t = 20$ ms. After that, the center of spherical flame moved upward in the combustion chamber. The movement of the flame center was caused by buoyancy.

Fig. 5 shows schlieren images of ammonia/air premixed flames with an equivalence ratio of $\phi = 1.0$ at the examined initial mixture pressure conditions. As the initial mixture pressure increased, the size of spherical flame became smaller. It could be concluded that the flame speed decreases with the increase in initial mixture pressure.

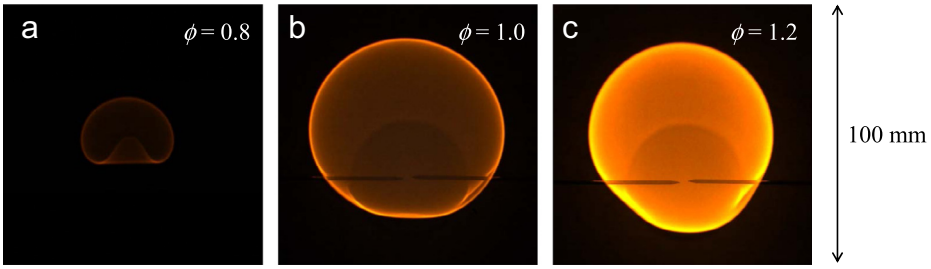

Fig. 2. Direct photographs of ammonia/air premixed flames of $P_i = 0.1$ MPa at $t = 100$ ms. (a) $\phi = 0.8$, (b) $\phi = 1.0$, (c) $\phi = 1.2$.

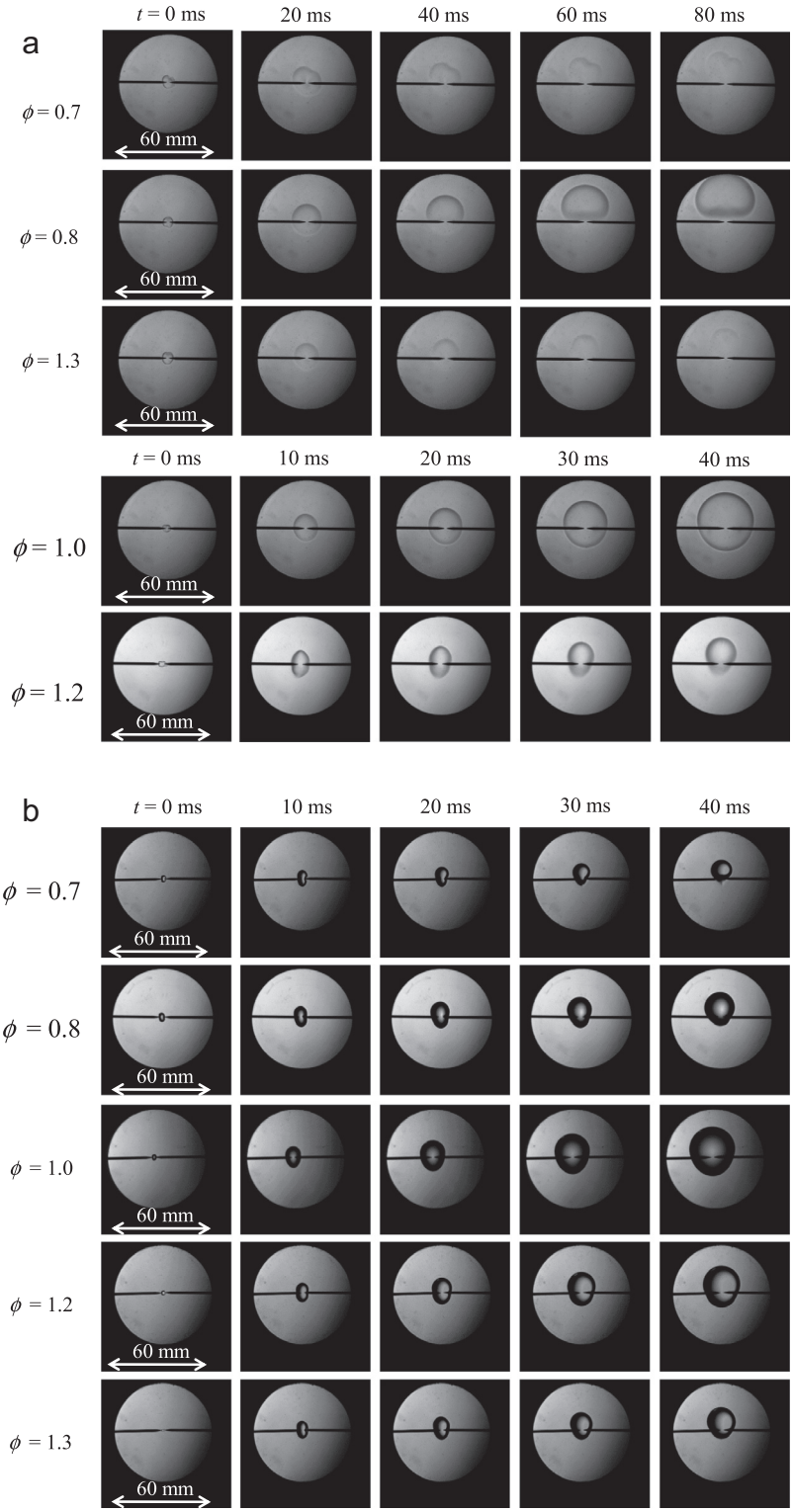

Fig. 4. Schlieren images of ammonia/air premixed flames (a) P_i = 0.1 MPa and (b) P_i = 0.5 MPa.

4.2. Unstretched laminar burning velocity and Markstein length

Fig. 6 shows the relationship between the stretched flame speed, S_N, and the flame stretch rate, ε, of a stoichiometric mixture at P_i = 0.1 MPa. Flame propagation in a constant volume combustion chamber can be classified into three periods: an ignition affected period, a quasi-steady period and a chamber affected period [20]. The quasi-steady period is shown by closed symbols in Fig. 6.

As flame propagated, flame stretch rate decreased, and then, flame speed rapidly increased at about $\varepsilon = 43\ s^{-1}$. Since the inner diameter of the chamber was sufficiently large, compared with the observation range, the influence of the chamber is considered to be small. As described in Section 4.1, the flame speed of

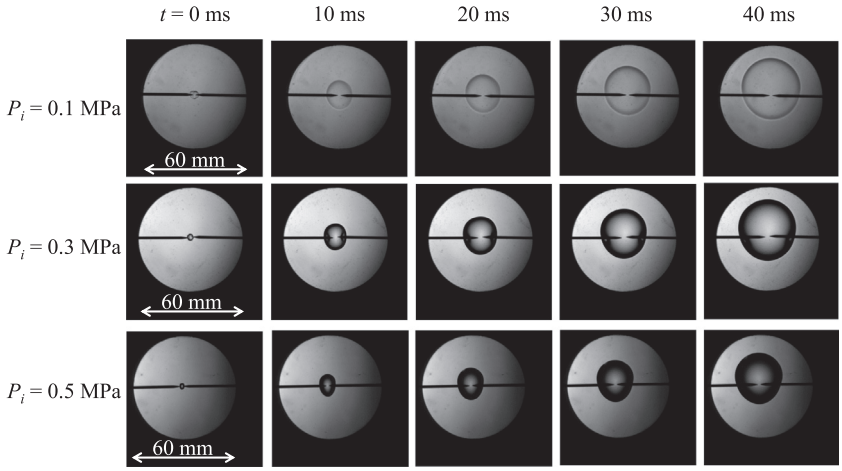

Fig. 5. Schlieren images of ammonia/air premixed flames at $\phi = 1.0$.

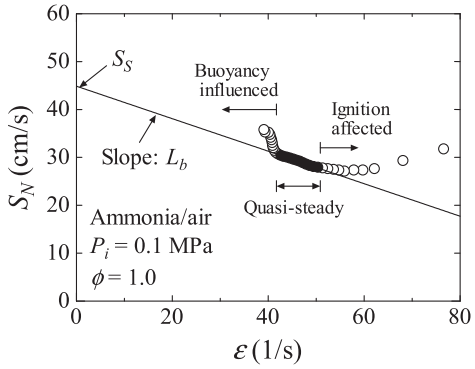

Fig. 6. Relationship between stretched flame speed, S_N, and flame stretch rate, ε.

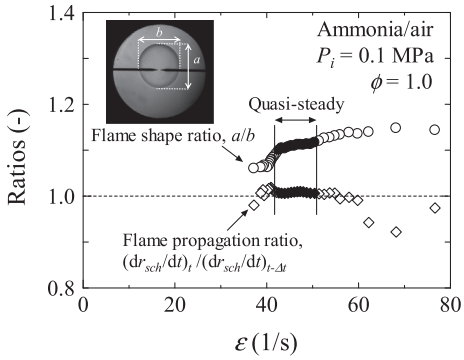

Fig. 7. Variations of flame shape ratio, a/b, and moving average of flame propagation ratio, $(dr_{sch}/dt)_t/(dr_{sch}/dt)_{t-\Delta t}$.

ammonia/air flames is very slow and thus flame shape changes from spherical flame owing to buoyancy. Therefore, the change in the flame speed is caused by the buoyancy, and thus the regime should be termed as a buoyancy influenced regime. In this study, the transitions of the ignition affected regime to a quasi-steady regime and the quasi-steady regime to a buoyancy influenced regime were determined based on the flame shape and the ratio of flame propagation speed. Here, the flame shape ratio and flame propagation ratio are defined as a/b and $(dr_{sch}/dt)_t/(dr_{sch}/dt)_{t-\Delta t}$, respectively. a and b are the length of the vertical and horizontal diameters of the flame, respectively. $(dr_{sch}/dt)_t$ denotes the flame propagation speed at time t. Since the frame rate of schlieren photography was 1000 fps in this study, Δt was 1 ms.

Fig. 7 shows the variations of the flame shape ratio and the moving average of the flame propagation ratio with the flame stretch rate at $P_i = 0.1$ MPa and $\phi = 1.0$. As shown in Fig. 7, in the regime which can be presumed to be a quasi-steady regime, the change in the flame shape ratio and the flame propagation ratio does not fluctuate so much. In this study, the quasi-steady regime was determined to be a regime in which the flame shape ratio and the moving average of the flame propagation ratio change smoothly. The time when the flame kernel starts the upward motion in the chamber does not correspond to the time when the flame propagation stage transitions to the buoyancy influenced regime. Although the upward movement of the flame kernel influences the propagation speed, it was considered that the influence of the upward motion was not significant. As shown in Fig. 6, the change in the stretched flame propagation speed, S_N, was well

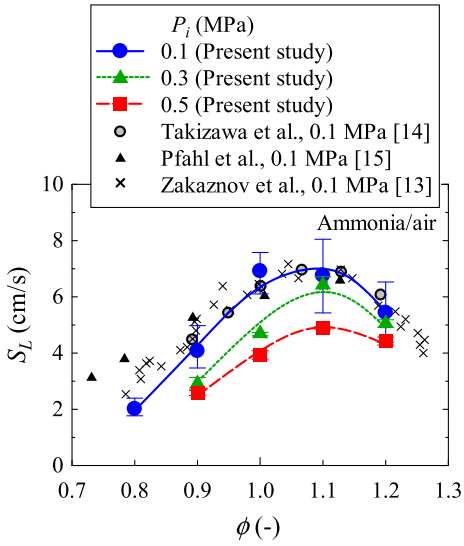

Fig. 8. Experimental and numerical results of the relationship between unstretched laminar burning velocity, S_L, and equivalence ratio, ϕ.

proportional to the flame stretch rate. Thus, the linear approximation by Eq. (3) was applied for the relationship between S_N and ε.

Fig. 8 shows the relationship between unstretched laminar burning velocity, S_L, and equivalence ratio, ϕ. The unstretched

laminar burning velocity reached its maximum value around an equivalence ratio of $\phi = 1.1$ for all examined initial mixture pressure conditions in this study. These tendencies are the same as those of hydrocarbon flames. The maximum value of the unstretched laminar burning velocity at the initial mixture pressure of 0.1 MPa was about 7 cm/s and was very low compared with that of hydrocarbon flames whose maximum value of the unstretched laminar burning velocity is about 35 cm/s. Although the flame propagated throughout the chamber at $\phi = 0.7$, 0.8 and 1.3 at $P_i = 0.3$ MPa and 0.5 MPa, the unstretched laminar burning velocity could not be evaluated owing to the significant influence of buoyancy because it is presumed that the unstretched laminar burning velocity is very low at these conditions.

The results obtained experimentally by Takizawa et al., Pfahl et al. and Zakaznov et al. are also plotted in Fig. 8. Even though the effects of flame stretch were not considered in the previous results, the laminar burning velocities are close to the results obtained in this study. As shown in Table 2, the Lewis number of ammonia/air premixed flames is close to unity. Therefore, the flame stretch, i.e., the thermo-diffusive effects, does not change significantly in unstretched laminar burning velocity. The unstretched laminar burning velocity decreased with the increases in the initial mixture pressure for all examined equivalence ratios.

Fig. 9 shows the variations of the burned gas Markstein length, L_b, with the equivalence ratio, ϕ. The burned gas Markstein length increases with the increase in the equivalence ratio. The tendency of the burned gas Markstein length is the same as those of hydrogen/air [32] and methane/air [33], but different from that of iso-octane/air [33]. The values of burned gas Markstein lengths at $\phi = 0.8$ and 0.9 are negative. As shown in Table 2, the Lewis numbers of ammonia/air flames of a lean mixture are lower than unity. Thereby, the burned gas Markstein lengths at lean mixtures are negative because temperature and burning velocity of stretched flames increase owing to the thermo-diffusive effects. Although the value of the burned gas Markstein length at $P_i = 0.1$ MPa is larger than that of 0.3 and 0.5 MPa, its values at $P_i = 0.3$ MPa and 0.5 MPa are almost the same.

Fig. 10 shows the relationship between preheating zone thickness, δ_l ($=\alpha/S_L$), and the equivalence ratio, ϕ. The preheating zone thickness is thinnest at the equivalence ratio of $\phi = 1.1$ for all initial mixture pressures because the unstretched laminar burning velocity was the fastest at this equivalence ratio. The preheating zone thickness decreases with the increase in initial mixture pressure. The preheating zone thicknesses of methane/air premixed flames obtained by Kitagawa [21] are also plotted in Fig. 10. The preheating zone thicknesses of methane/air flames are thinner than those of ammonia/air premixed flames because unstretched laminar burning velocities of methane/air flames are faster than those of the ammonia/air premixed flames.

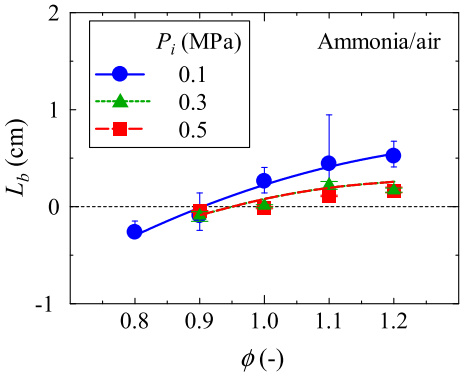

Fig. 9. Relationships between burned gas Markstein length, L_b, and equivalence ratio, ϕ.

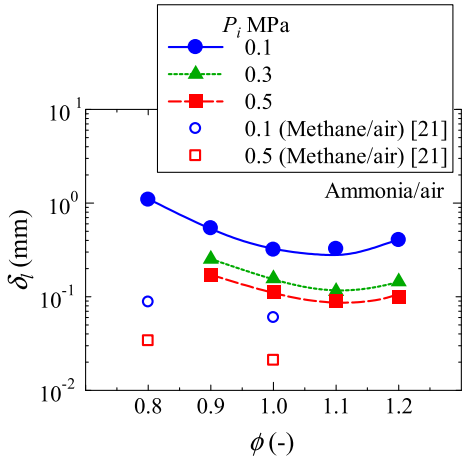

Fig. 10. Relationships between preheating zone thickness, δ_l, and equivalence ratio, ϕ.

The Lewis number of ammonia/air flames and that of methane/air flames are almost unity and the variation of Lewis number with the equivalence ratio of ammonia/air flames and that of methane/air flames are similar. In the case of the turbulent combustion, which is used in actual combustors, the thermo-diffusive effect is important for turbulent flame characteristics. Because the variation of Markstein length of ammonia/air flames and that of methane/air flames are similar, the turbulent flame characteristics are considered to be similar from the standpoint of thermo-diffusive effects. According to the Peters regime diagram [34], flame thickness is an important parameter of turbulent flame structures. Thus, the flame structure is considered to be different because the laminar flame thickness is significantly different.

Fig. 11 shows the variation of unstretched laminar burning velocity, S_L, with the initial mixture pressure, P_i, at the equivalence ratios of (a) $\phi = 0.9$, (b) $\phi = 1.0$ and (c) $\phi = 1.2$, respectively. The results of numerical simulation by CHEMKIN-PRO with detailed reaction mechanisms are also plotted in Fig. 11. The calculated unstretched laminar burning velocity decreases with the increase in initial mixture pressure and is the same tendency as that of the experimental results. The calculated unstretched laminar burning velocity decreases in the order of Konnov, Lindstedt and Miller, Tian, and GRI-Mech 3.0. Most numerical simulations overpredict when compared with the experimental results. Although the results from GRI-Mech 3.0 seem to be close to the experimental results, GRI-Mech 3.0 is possibly not appropriate for the numerical simulation of ammonia flames because N reactions including NO and NH_2 reactions are insufficient.

Although some of these reactions take the ammonia reaction into consideration and are used in the study of ammonia/hydrogen/air flames [5], they have not been optimized for the ammonia/air combustion. The detailed chemical kinetics of Tian's mechanism [12] was developed based on $NH_3/CH_4/O_2/Ar$ flame at a reduced pressure condition in order to identify the detailed flame structure using tunable synchrotron vacuum ultraviolet photoionization and molecular-beam mass spectrometry. Konnov's mechanism [11] was responsible for the prompt NO formation from hydrocarbon flames. Although the detailed chemical kinetics of Lindstedt's mechanism [10] and Miller's mechanism [9] were developed based on ammonia combustion, these mechanisms were developed considering NH_3/O_2, $NH_3/H_2/O_2$, $NH_3/NO/O_2$ and $NH_3/NO/O_2/H_2/Ar$ flames to permit comparison with the previous experimental results. GRI-Mech [26] was optimized for natural gas combustion. Therefore, further improvement of the ammonia reaction mechanisms is essential.

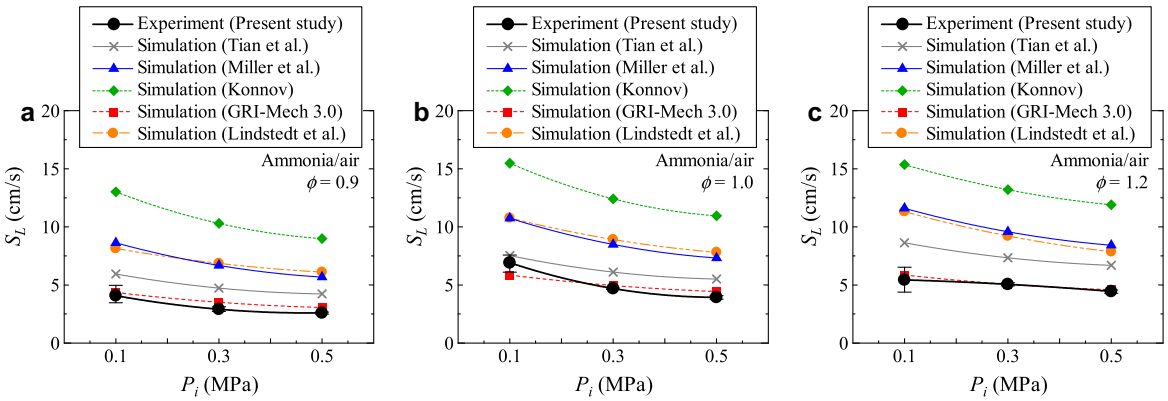

Fig. 11. Variations of unstretched laminar burning velocity, S_L, with initial mixture pressure, P_i. (a) ϕ = 0.9, (b) ϕ = 1.0, (c) ϕ = 1.2. The numerical simulations were conducted with detailed chemical kinetics developed by Miller et al. [9], Lindstedt et al. [10], Konnov [11], and Tian et al. [12] and with GRI-Mech 3.0 [26]. Here, all carbon reactions were removed from Konnov's mechanisms.

5. Conclusions

The laminar burning velocity and the burned gas Markstein length of the ammonia/air premixed flames were experimentally investigated at the various pressures up to 0.5 MPa. Spherically propagating premixed flames, which propagated in a constant volume combustion chamber, were observed using high-speed schlieren photography. The equivalence ratio was varied from 0.7 to 1.3. Numerical simulation using five detailed reaction mechanisms, which can be applied to ammonia flames, were also conducted. The following results were obtained:

1. The maximum laminar burning velocity reaches its peak value around an equivalence ratio of 1.1 for all examined initial mixture pressure conditions. Unstretched laminar burning velocity of ammonia/air premixed flames decreases with an increase in the initial mixture pressure. That tendency is the same as that of hydrocarbon fuels.
2. The burned gas Markstein length increases with an increase in equivalence ratio. This tendency is the same as that of methane/air and hydrogen/air flames. The burned gas Markstein lengths of lean flames at an initial mixture pressure of 0.1 MPa are negative. The burned gas Markstein lengths at elevated pressures of 0.3 MPa and 0.5 MPa are lower than those of 0.1 MPa. However, the values of burned gas Markstein length at 0.3 MPa and 0.5 MPa are also the same.
3. Reaction mechanisms used in this study can predict the qualitative variation of the unstretched laminar burning velocity with the initial mixture pressure, i.e., the unstretched laminar burning velocity decreases with the increase in the initial mixture pressure. However, those mechanisms are not applicable for quantitative prediction of unstretched laminar burning velocity. Thus, further improvement of reaction mechanisms of the ammonia/air flames is essential.

Acknowledgements

This research was supported by the Council for Science, Technology and Innovation (CSTI), the Cross-ministerial Strategic Innovation Promotion Program (SIP), "Energy Carrier" (Funding agency: the Japan Science and Technology Agency (JST)).

References

[1] Chiuta S, Everson RC, Neomagus HWJP, Van der Gryp P, Bessarabov DG. Reactor technology options for distributed hydrogen generation via ammonia decomposition: a review. Int J Hydrogen Energy 2013;38:14968–91.
[2] Michalsky R, Rarman BJ, Amanor-Boadu V, Pfromm PH. Solar thermochemical production of ammonia from water, air and sunlight: thermodynamic and economic analyses. Energy 2010;42:251–60.
[3] Lee JH, Kim JH, Park JH, Kwon OC. Studies on properties of laminar premixed hydrogen-added ammonia/air flames for hydrogen production. Int J Hydrogen Energy 2010;35:1054–64.
[4] Lee JH, Lee SI, Kwon OC. Effects of ammonia substitution on hydrogen/air flame propagation and emissions. Int J Hydrogen Energy 2010;35:11332–41.
[5] Kumar P, Meyer TR. Experimental and modeling study of chemical-kinetics of mechanisms for H_2–NH_3–air mixtures in laminar premixed jet flames. Fuel 2013;108:166–76.
[6] Frigo S, Gentili R, Doveri N. Ammonia plus hydrogen as fuel in a S.I. engine: experimental results. SAE paper; 2012 [2012-32-0019].
[7] Frigo S, Gentili R. Analysis of the behaviour of a 4-stroke Si engine fuelled with ammonia and hydrogen. Int J Hydrogen Energy 2013;38:1607–15.
[8] Hayakawa A, Goto T, Mimoto R, Kudo T, Kobayashi H. NO formation/reduction mechanisms of ammonia/air premixed flames at various equivalence ratios and pressures. Mech Eng J 2015;2:14–00402.
[9] Miller JA, Smooke MD, Green RM, Kee RJ. Kinetic modeling of the oxidation of ammonia in flames. Combust Sci Technol 1983;34:149–76.
[10] Lindstedt RP, Lockwood FC, Selim MA. Detailed kinetic modelling of chemistry and temperature effects on ammonia oxidation. Combust Sci Technol 1994;99:253–76.
[11] Konnov AA. Implementation of the NCN pathway of prompt-NO formation in the detailed reaction mechanism. Combust Flame 2009;156:2093–105.
[12] Tian Z, Li Y, Zhang L, Glarborg P, Qi F. An experimental and kinetic modeling study of premixed NH_3/CH_4/O_2/Ar flames at low pressure. Combust Flame 2009;156:1413–26.
[13] Zakaznov FZ, Kursheva LA, Felina ZI. Determination of normal flame velocity and critical diameter of flame extinction in ammonia–air mixture. Combust Explos Shock Waves 1978;14:710–3.
[14] Takizawa K, Takahashi A, Tokuhashi K, Kondo S, Sekiya A. Burning velocity measurements of nitrogen-containing compounds. J Hazard Mater 2008;155:144–52.
[15] Pfahl UJ, Ross MC, Shepherd JE, Pasamehmetoglu KO, Unal C. Flammability limits, ignition energy, and flame speeds in H_2–CH_4–NH_3–N_2O–O_2–N_2 mixtures. Combust Flame 2000;123:140–58.
[16] Williams FA. Combustion theory. 2nd ed. California: Benjamin/Cummings Publishing; 1985.
[17] Kitagawa T, Nakahara T, Maruyama K, Kado K, Hayakawa A, Kobayashi S. Turbulent burning velocity of hydrogen–air premixed propagating flames at elevated pressures. Int J Hydrogen Energy 2008;33:5842–9.
[18] Hayakawa A, Takeo T, Miki Y, Nagano Y, Kitagawa T. Study of thermo-diffusive effects on iso-octane/air flames at fixed turbulence Karlovitz number. In: Proc 8th AJTEC; 2011 [AJTEC2011-44221].
[19] Tse SD, Zhu DL, Law CK. Morphology and burning rates of expanding spherical flames in H_2/O_2/inert mixtures up to 60 atmospheres. Proc Combust Inst 2000;28:1793–800.
[20] Kelley AP, Law CK. Nonlinear effects in the extraction of laminar flame speeds from expanding spherical flames. Combust Flame 2009;156:1844–51.
[21] Kitagawa T. Effects of pressure on burning velocity and instabilities of propane-air premixed flames. JSME Int J Ser B 2005;48:2–8.
[22] Kobayashi H, Otawara Y, Wang J, Matsuno F, Ogami Y, Okuyama M, et al. Turbulent premixed flame characteristics of a CO/H_2/O_2 mixture highly diluted with CO_2 in a high-pressure environment. Proc Combust Inst 2013;34:1437–45.
[23] Bradley D, Lawes M, Liu K, Mansour MS. Measurement and correlations of turbulent burning velocities over wide ranges of fuels and elevated pressures. Proc Combust Inst 2013;34:1519–26.
[24] Lewis B, Von Elbe G. Combustion, flames and explosions of gases. 3rd ed. London: Academic Press; 1987.
[25] CHEMKIN-PRO Release 15101. Reaction Design; 2010.

[26] Frenklach M, Bowman T, Smith G. GRI-Mech 3.0. 2000. <http://www.me.berkeley.edu/gri-mech/index.html>.
[27] Clavin P. Dynamic behavior of premixed flame fronts in laminar and turbulent flows. Prog Energy Combust Sci 1985;11:1–59.
[28] Matalon M. On flame stretch. Combust Sci Technol 1983;31:169–81.
[29] Pearse RWB, Gaydon AG. The Identification of molecular spectra. 4th ed. New York: John Wiley & Sons, Inc; 1976.
[30] Law CK. Combustion physics. New York: Cambridge University Press; 2006.
[31] Ballal DR, Lefebvre AH. The influence of spark discharge characteristics on minimum ignition energy in flowing gases. Combust Flame 1975;24:99–108.
[32] Hu E, Huang Z, He J, Miao H. Experimental and numerical study on laminar burning velocities and flame instabilities of hydrogen–air mixtures at elevated pressures and temperatures. Int J Hydrogen Energy 2009;34:8741–55.
[33] Varea E, Modica V, Vandel A, Renou B. Measurement of laminar burning velocity and Markstein length relative to fresh gases using a new postprocessing procedure: application to laminar spherical flames for methane, ethanol and isooctane/air mixtures. Combust Flame 2012;159:577–90.
[34] Peters N. Turbulent combustion. Cambridge: Cambridge University Press; 2000.